Galvanic Corrosion of Carbon Steel -Stainless Steel Couple in Sulfuric Acid under Flow Conditions

Basim Obed Hasan
Assistant Professor
Chemical Eng. –Nahrain University
Email: basimohasan13@gmail.com

Naseer Abood Al-habubi
Assistant Professor
Chemical Eng. -Nahrain University
Email: naseer@habobi.com

Samar Saadi Hussien
Ph. D student
Chemical Eng. - Nahrain University
Email: samar_saadi@yahoo.com

ABSTRACT

Galvanic corrosion of stainless steel 316 (SS316) and carbon steel (CS) coupled in 5% wt/v sulfuric acid solution at agitation velocity was investigated. The galvanic behavior of coupled metals was also studied using zero resistance ammeter (ZRA) method. The effects of agitation velocity, temperature, and time on galvanic corrosion current and loss in weight of both metals in both free corrosion and galvanic corrosion were investigated. The trends of open circuit potential (OCP) of each metal and galvanic potential (E_g) of the couple were, also, determined. Results showed that SS316 was cathodic relative to CS in galvanic couple and its OCP was much more positive than that of CS for all investigated ranges of operating conditions. A sharp increase in galvanic current from CS to SS316 was noticed in the first 20 min and then decrease with time. Increasing the agitation velocity led to increase in galvanic corrosion rate. The decrease in galvanic current is attributed to metal passivation due to the formation of a protective film which grows with time. The minus sign in galvanic current means that the current is flow from CS (anode) to SS316 (cathode). The galvanic current of CS-SS316 couple shifts to the negative direction with increase agitation velocity.

Keywords: Galvanic current; corrosion rate; potential; passivation film.

التاكل الكلفاني للحديد الكاربوني والحديد المقاوم للصدأ في حامض الكبريتيك تحت تاثير الجريان

ا. م.د. باسم عبيد حسن
هندسة كيمياوية/ جامعة النهرين

ا.م.د. نصير عبود الحبوبي
هندسة كيمياوية/ جامعة النهرين

سمر سعدي حسين
هندسة كيمياوية/ جامعة النهرين

الخلاصة

تم دراسة التاكل الكلفاني للحديد الكاربوني والحديد المقاوم للصدأ بوجود سرع في (5% wt/v) حامض الكبريتيك. السلوك الكلفاني للمعدنين ايضا درس باستعمال مقياس التيار الكهربائي ذو المقاومة صفر (ZRA) . تاثير السرعة ودرجة الحرارة والزمن على تيارات التاكل الكلفاني والوزن المفقود للمعدنين في حالة التاكل الحر والتاكل الكلفاني. حساب جهود المعادن في الحالة الحرة والربط الكلفاني. من النتائج نلاحظ ان الحديد المقاوم للصدأ هو كاثود الحديد الكاربوني هو انود في حالة الربط الكلفاني. الجهد الحر للحديد المقاوم للصدأ في جميع الظروف المدروسة كان اكثر خمولا من الحديد الكاربوني. زيادة حادة في التيار الكلفاني من الحديد الكاربوني الى الحديد المقاوم للصدأ في اول عشرين دقيقة ثم يقل مع الزمن وهذا يزداد مع زيادة السرعة. نقصان معدل التاكل الكلفاني وكذلك معدل التاكل الحر للحديد المقاوم وذلك بسبب تاثير طبقة الحماية على سطح المعدن التي تنمو مع الزمن. الاشارة السالبة في التيارالكلفاني تعني اتجاه التيار من الحديد الكاربوني الى الحديد المقاوم.تزداد قيمة التيار الكلفاني للمعدنين معا باتجاه السالب (وذلك يعني الحديد الكاربوني انود والحديد المقاوم للصدأ هو كاثود) مع زيادة السرعه.

الكلمات الرئيسية: التيار الكلفاني, معدل التاكل ,الجهد, طبقة الحماية.

1. INTRODUCTION

Galvanic corrosion occurs when two dissimilar metals, with different potentials, in electrical contact are exposed to an electrically conducting corrosive liquid, because the metals have different natural potentials in the liquid, a current will flow from the anode (more electronegative) metal to the cathode (more electropositive), the less noble metal in general suffers more corrosion and the more noble metal suffers less than if they were isolated in the same medium **Talbot**, and **Talbot, 1998**.

Acidic solutions of hydrochloride acid and sulfuric acid have wide industrial applications, the most important fields being acid pickling, acid descaling, industrial cleaning and oil-well acidizing. In aqueous solutions of acids, the surface of metals and alloys are covered with highly protective oxyhydroxide passive film affecting its corrosion behavior **Singh**, and **Ray, 2007**.

The corrosion behavior of carbon steel in acidic solution is significant considering its widespread applications, namely, in the manufactures of pipe lines for petroleum industries. Acid solutions are frequently used in the removal of rust and scale-developed in industrial process. Since the steel is the major structural material utilized in the construction industry, there have been considerable efforts focused on the prevention of steel corrosion. As most steels are stable in neutral or alkaline media, acidic environments are the major concern. However, a group of materials that could serve as substitutes of steel are the inter metallic compounds when exposed to acidic solutions because these compounds possess good corrosion and oxidation resistance in media, containing not only oxygen but also sulphur, good abrasion resistance, and small density **Greene et al, 1961; Guo et al, 1986; Higginson et al, 1989; Hermas et al, 1995**.

Since stainless steels are passive and exhibit a noble potential, they can be coupled successfully to metals that are either passive or inherently noble. This includes metals and alloys like silver; silver solder; copper; nickel; 70% Ni − Cu alloy; 76% Ni, 16% Cr, 7% Fe alloy; and, usually, aluminum in environments in which it remains passive. Stainless steels are best employed under fully aerated or oxidizing conditions, which favor the passive state. Whether used in handling chemicals or exposed to the atmosphere, the alloy surface should always be kept clean and free of surface contamination **Revie** and **Uhlig, 2008**.

Stainless steels are more resistant to concentrated sulfuric acid than carbon steels. Because the passive film on stainless steel is harder and much more resistant to flow-induced corrosion than is the iron sulfate film which form on carbon steels, use of corrosion resistant alloys for components such as valves, inlets, outlets, and wear plates is advised in the standard. Application for stainless steel in sulfuric acid production is in towers, pumps, tanks, mist eliminators, acid coolers, and piping **Grubb, 2009**.

To control the corrosion, good understanding of the effect of operating conditions on the corrosion behavior is required. Therefore, this work aims to study free corrosion and galvanic corrosion behavior of carbon steel and stainless steel in sulfuric acid for ranges of temperatures and agitation speed. Then, galvanic current between each couple of these metals will be investigated under the same conditions by using zero resistance ammeter and also by weight loss. Potential measured of each metal to study the free corrosion behavior, whereas, the galvanic currents will be measured using zero resistance ammeter (ZRA). The galvanic coupling effect on the corrosion behavior of metal is important to be investigated. The loss in weight of coupled metals is necessary to be determined before and after coupling.

2. EXPERIMENTAL WORK

The free corrosion rate for specimens CS and SS316 was determined by weight loss method under agitation velocity of 0, 400, and 600 rpm, and temperatures 30, 40, 50 and 60 ºC, in a solution of 5% wt/v H_2SO_4. And the galvanic corrosion rate of CS-SS316 couple was evaluated under isothermal (T=40 °C) and agitation velocity 0, 400, and 600 rpm.

Fig. 1 shows the connected experimental apparatus that was used in galvanic experiments. The corrosion rate for two dissimilar metals was calculated by measured weight loss before and after experiment.

The electrode specimens were mechanically press-cut into coupons of 20 mm ×40 mm dimensions with a total specimen surface area of 800 mm^2. The specimen were connected to a plastic board through a very small holes made in the center using fine screw. The effect of screw was ignored. The chemical composition of specimen is shown in **Table 1** and **2**.

Before each experiment the specimen was abraded with glass emery paper of grade numbers; 120, 180, 220, 400 and 2000 respectively, washed continuously with brushing by plastic brush in running tap water, followed by distilled water, dried with a clean tissue, followed by ethanol for 30 second dried with clean tissue, and then dried by using electrical oven to temperature of about 110 ºC for 10 minute **Mahato et al., 1980**. The specimen then was stored in the desiccator over high activity silica gel until use.

Then the specimen was weighed to the 4th decimal of gram by using digital balance. After that one face of the rectangular coupon was exposed to corrosion environment for 1 h by immersion in acid solutions, while the other face was completely insulated by insulating tape. So that the corrosion rate of each specimen was determined for two cases: free corrosion and galvanic corrosion.

At the end of weight loss experiment, the specimen was washed by tap water with brushing to remove the corrosion products that may still stick to surface, washed with distilled water, dried with clean tissue, rinsed in ethanol and dried by using electrical oven to a temperature about 110 ºC for 10 minute. Then the specimen was kept in the desiccator to cool and then weighted. The change in the open circuit potential of specimen as function of time was measured at the all weight loss experimental run.

In galvanic corrosion experiments, before each experiment, the specimens were weighed by accurate balance. After the solution had reached the required isothermal temperature and velocity, the two dissimilar metals were connected together to measure galvanic currents variation with time by using Zero Resistance Ammeter (ZRA). The carbon steel specimen was connected to the (+ve) and the stainless steel to the (-ve). The distance between the specimens in the test solution was maintained at 10 mm in all experiments. The coupons were mounted by connecting them on hold board using a small screw.

During each experimental run, galvanic potential variation with time was measured by using Saturated Calomel Electrode SCE bridged by a Luggin capillary at a distance of 1- 2 mm from the working electrode, and connected to personal computer for data recording. The specimens were immersed in the acid solution for 1 h. During this time period, the galvanic current and potential were measured with time. After each run, the couple specimens were weighed by high accuracy balance. Each run was repeated twice, a third run was conducted in case of any doubt in the results.

3. RESULTS AND DISCUSSION

3.1 Free corrosion

Fig. 2 and **3** illustrates the variation of corrosion rate of carbon steel (CS) and stainless steel 316 (SS316) that expressed in gmd with temperature and flow velocity for a 1 h of immersion time.

From **Fig. 2** it is clear that the corrosion rate increases with increasing temperature for both metals at the stationary condition. The effect of temperature on the corrosion rate is governed by changing two parameters affecting the corrosion rate in conflicting ways that are the O_2 solubility and diffusivity. Increasing the temperature will increase the rate of oxygen diffusion to the metal surface by decreasing the viscosity of aqueous solutions resulting in enhanced corrosion rate. On the other hand, increasing temperature decreases the oxygen solubility the factor that restrains the corrosion **Mahato et al, 1980**. It is also evident from **Fig. 2** that the increase in the CR of SS is very little with increasing temperature. This agrees with previous works **Okamoto, 1973; Grubb, 2009; Ibrahim et al, 2015**.

From **Fig. 3**, it is clear that increasing the flow velocity leads to an increase in the corrosion rate of CS while the influence on the SS corrosion is negligible. This can be attributed to the increase in the concentration of oxygen close to the metal surface by eddy transport. The rate of oxygen reduction reaction is generally limited by the speed at which oxygen can reach the surface of the metal. Previous studies **Foroulis, 1979; Scheers, 1992; Shreir et.al, 2000; Slaiman and Hasan, 2010; Hasan and Sadek, 2014** indicated that the greater the turbulence due to high velocities results in more uniform O_2 concentration near the surface. **Figs 2** and **3** reveal that the corrosion rate of CS exhibited high corrosion rate compared to stainless steel. In addition, their corrosion rates increased appreciably with temperature. Stainless steel exhibited a clear corrosion resistance under most investigated conditions even at high temperature and high rotational speed. This is due to the increased anodic polarization and a possibility of passivation.

Fig. 4 and **5** shows the corrosion potential (open circuit potential) versus time for carbon steel and stainless steel respectively in 0.52 M H_2SO_4 solutions at four different temperatures of 30, 40, 50, and 60 ºC, for stationary condition. From **Fig. 4** for CS, it is clear that the potential at 30 and 40 ºC shifts to more negative and reaching asymptotic values of -0.566 and -0.524 V respectively after about 10 min.

At 50 and 60 ºC, the potentials show a decrease of the corrosion potential value and then after 4 and 10 min respectively the potential shifts towards more positive until reach stable value is -0.524 and -0.507 V after 1 h. This shift can be ascribed to the formation and growth of a Fe_2O_3 film on the corroding surface. The ennoblement of the potential observed in **Fig. 4** is attributable to healing of the pre-immersion air-formed oxide film and further thickening of the oxide film as a result of the interaction between the electrolyte and the metal surface **Evan, 1960**. The growth of the oxide film continues until the film acquires a thickness that is stable in the electrolyte. During this step the alloy oxidation is under anodic control and the reduction of oxygen is the cathodic reaction **Abd El Kader**, and **Shams El Din, 1979**.

Fig. 5 for SS316, at 30 ºC the potential shifts to the negative values in the first 13 min and then slow increase in potential. At 40 ºC the potential decreases in the first 4 min and then shifts to the positive value in the four minute and tends to more positive in the 20 min. At 50 ºC the potential decrease in the first 5 min and then increases until it reaches stable value (E_{corr}= -0.46 V) in 30 min. At 60 ºC initial potential increases in the first 8 min and then reaches stable value at E_{corr}= -0.405V. The asymptotic values (steady state values) and the OCP increases with increasing temperature. The potential profiles can be explained by assuming that the potential rise indicates the formation of an insoluble layer product, probably oxide phase on the electrode surface. The anodic shifting of E_{corr} can be attributed to the product layer thickening process and to an increase in the resistance of this layer. These results are in agreement with **Alain et al., 2013** for 316L stainless steel in HCl aqueous solution, **Azambuja et al., 2003** for Fe and AISI 304 stainless steel in tungstate aqueous solution, and with **Bore et al., 2006** for 304 stainless steel in sulfuric acid.

The temperature favors the cathodic reaction and more specifically, it favors the hydrogen evolution reaction (HER) which leads to an increase of H_2 evolution. In other words, an increase of temperature decreases the cathodic overpotential as a result of decreasing the activation overpotential of hydrogen evolution reaction. Moreover, temperature also favors the kinetics of the corrosion reactions, and especially the anodic dissolution of the alloy, since the corrosion current densities are high for each alloy as temperature increases **Ibrahim et al, 2015**.

It is worth to mention that the passive region appeared on the anodic region of the polarization curves for iron and steel was due to the formation of iron oxides and/or corrosion products on their surfaces as shown by Equations (1) and (2) **Sherif, 2014**.

$$Fe + ½\ O_2 + H_2O = Fe(OH)_2 \quad (1)$$

$$3Fe(OH)_2 + ½\ O_2 = Fe_3O_4 + 3H_2O \quad (2)$$

where, the formed ferrous hydroxide reacted with more oxygen to form the top layer of magnetite corrosion product, Fe_3O_4. The presence of such oxide partially protects the iron surface from further dissolutions and led to the appearance of the passive region **Sherif, 2014**.

Shams El Din et al., 1994 demonstrated that the surface of high molybdenum containing stainless steel immersed in seawater at high temperatures becomes rich with molybdenum ions due to outward diffusion of molybdenum ions through the oxide film as confirmed by X-ray surface analysis. Therefore, the behavior indicated in **Fig. 6** can be attributed to the dissolution of the passive film on the steel in the temperature ranging from 30 to 40 °C and 50 to 60 °C is under mixed control (anodic and cathodic). While in the range of 40 to 50 °C, the oxygen solubility in the solution decreases with increasing temperature, so the passivation process becomes under cathodic control.

Fig. 7 and **8** shows the effect of agitation speed on the corrosion potential curves vs. time of carbon steel and stainless steel 316 respectively, in 0.52 M H_2SO_4 solution at isothermal temperature T=40 ºC for 1 h immersion time.

Fig. 7 for CS reveals that when the velocity increases from 0 to 400 rpm, the potential shifts to more negative. This is due to increased arrival O_2 to the metal surface which leads to an increase in the polarization resistance to more negative values. The corrosion potential shifts to more positive (higher than 400 rpm) when the velocity up to 600 rpm.

Fig. 8 for SS316 shows that the potential shifts to more positive values with increasing velocity due to the increased O2 transport to the surface. This agrees with previous findings **Foroulis, 1979; Mahato et al, 1980; Silverman, 1984; Hasan, 2003; Hasan et al, 2011**. Therefore, the corrosion potential in aerated and oxygen-saturated solutions is flow dependent since the cathodic process, i.e., oxygen reduction reaction, is mass transfer controlled, i.e., at a constant bulk temperature the corrosion potential (E_{corr}.) increases as the flow rate increases. The anodic kinetics (dissolution of metal) is not mass transfer dependent as it is under activation control. The oxygen reduction reaction is dictated by the limiting values of mass transfer control. This may explain the noble trend of the corrosion potential as the flow rate (rpm) is increased as in **Fig. 8**. This behavior is in agreement with previous findings **Hubbard** and **Lightfoot, 1966; Chin** and **Nobe, 1977; Nesic et.al, 1995; Ross et al, 1966**. **Ross et al., 1966**, stated that the increase in E_{corr} with velocity is due to the increase in oxygen transport to the metal surface and when the system is free from oxygen, velocity has no effect on corrosion potential (E_{corr}).

3.2 Galvanic corrosion

Fig. 9 shows corrosion potential with time of CS, SS316, and CS–SS316 couple in a H_2SO_4 solution at 40 ºC for stationary conditions (u=0 rpm). It is clear that the OCP of CS and SS316 free reveals that the corrosion potential decreases and then increases after 5 min and more increases at 20 min decreases with time while the CS-SS316 couple initial rises in first few minutes and reaching almost steady value. Some of literature found the same tendency such as **Azambuja et al., 2003** for Fe & AISI 304 stainless steel in tungstate aqueous solution, **Bore et al., 2006** for 304 stainless steel in sulfuric acid, **Alain et al., 2013** for 316L stainless steel in HCl aqueous solution. **Fig. 9** reveals that OCP of CS is nobler than SS316 in the first 5 min. and reverse after that time. However, the galvanic potential of CS–SS316 couple is nobler than OCP of CS and SS316. The degree of passivity, the nature of the redox couples in the solution, and the stability of the system, all determine the polarity and its variation with time **Gilbert, 1948**.

During the OCP test the passive film containing Cr_2O_3 grew on the electrode surface, shifting the OCP value to higher potentials **Lothongkum et al, 2003**.

Fig. 10 and **11** shows a comparison of the potential variation with time for CS, SS316, and CS- SS316 couple in H_2SO_4 solution for agitation velocity of 400 and 600 rpm at T=40ºC respectively.

Fig. 10 for CS indicates that the OCP of CS and the galvanic potential become more negative with time. It reveals that OCP of SS316 is nobler than OCP of CS, whereas the galvanic potential of CS-SS316 couple is between the OCPs of the two metals.

Fig. 11 shows the galvanic potential of CS- SS316 couple and OCP of SS316 decrease and then increase in positive direction and the values of potentials are almost equal. However, the OCP of CS shifts to more negative direction.

Fig. 12 shows the effect of agitation speed on galvanic potential (CS- SS316 couple) at T=40ºC. It is clear from figure that the galvanic potential shifts toward the negative direction with increasing agitation velocity from 0 to 400 rpm. This indicates that the E_g is affected by the CS potential more than by SS316 potential. E_g goes to the positive direction when increasing the velocity from 400 to 600 rpm and that revels the E_g is affected by the SS316 potential due to passivation layer on SS316 surface at velocity 600 rpm higher than at 400 rpm. **Table 3** shows the corrosion rate of CS when coupled with SS316, at velocity 400 rpm it is less than that at 600 rpm suggesting that due to the galvanic potential at 600 rpm higher than 400 rpm.

Fig. 13 shows the variation of galvanic current of CS-SS316 couple with time for different agitation velocity at T=40 ºC. The minus sign in galvanic current means that the current is flowing from CS (anode) to SS316 (cathode). The figure reveals that there is a sharp increase in galvanic current from CS to SS316 in the first 20 min and then it decreases with time. It can be seen that the galvanic current increase with increasing velocity. The decrease in galvanic current is attributed to metal passivation due to the formation of a protective film which grows with time **Guenbour, 2010** this film increases with velocity.

The corrosion data for carbon steel-stainless steel 316 couple are summarized in **Table 3**. The direction of the galvanic currents shows that carbon steel is anodic (electronegative or corroding) pole of CS-SS316 couples immersed in 0.52 M H_2SO_4 solution. Since the open circuit potential of SS316 is higher than the open circuit potential of CS, the current flows from CS to SS316.

Table 3 lists the values of corrosion rate obtained from weight loss of CS and SS316 in both free and coupling cases for range of agitation velocity at constant temperature T=40 ºC. The values of corrosion rate reveal that the corrosion rate of SS316 is lower than that for CS and that indicate the SS316 is cathodic and CS is anodic in the galvanic couple. In addition, when coupling CS with SS316, the corrosion rate of SS316 decreases and that of CS increases due to the galvanic action. Under flow conditions, the corrosion rate of CS increases due to the galvanic effect produced by coupling with SS316, while the SS316 is protected. Under flow conditions at 600 rpm, the corrosion rate of carbon steel coupled to stainless steel 316 is lower than free corrosion of carbon steel. This may be attributed to the formed protective oxide film on carbon steel and become the sacrificial anode. Moreover, the galvanic potential of couple at 600 rpm is higher than that at 400 rpm. That justified the decrease in the galvanic current with increased velocity (from 400 rpm to 600 rpm).

4. CONCLUSIONS

1- The free corrosion rate for SS316 is lower than CS due to its passivity.

2- The galvanic current of CS-SS316 couple shifts to the negative direction with increase agitation velocity.

3- When coupling CS with SS316, the corrosion rate of SS316 decreases while the CS increases at stationary with negligible effect at agitation velocity.

4- The open circuit potential for CS shifts to more positive with increasing temperature and time (especially at high temperature) and, in general, to more negative with increasing agitation velocity.

5- The open circuit potential for SS316 shifts to more positive with increasing temperature, time and agitation velocity.

REFERENCES

- Abd El Kader, J.M. and Shams El Din, A.M., 1979, *Film thickening on nickel in aqueous solutions in relation to anions type and concentration*, Br. Corros. J., Vol. 14, PP. 40–45.

- Alain, R., Gilbert, S., Jorge, L. R., 2013, *Corrosion Behavior of HA-316L SS Biocomposites in Aqueous Solutions*, Materials Research, Vol. 16, No. 6, PP. 1254-1259.

- Azambuja, D. S., Emilse, M. A., Martinia, and Iduvirges L. M., 2003, *Corrosion Behaviour of Iron and AISI 304 Stainless Steel in Tungstate Aqueous Solutions Containing Chloride*, J. Braz. Chem. Soc., Vol. 14, No. 4, PP. 570-576.

- Bore J., Dragutin M. D. and Jovan P. P., 2006, *Corrosion potential of 304 stainless steel in sulfuric acid*, J. Serb. Chem. Soc. Vol. 71, No. 5, PP. 543–551.

- Chin, R. J., and Nobe, K., 1977, *Electrochemical aspects of Steel Corrosion in Sea Water*, Corrosion J., vol.33, pp.364.

- Evans, U.R., 1960, *The Corrosion and Oxidation of Metals*, Edward Arnold, London, PP. 898.

- Foroulis, Z. A., 1979, *The Influence of Velocity and Dissolved Oxygen on the Initial Corrosion Behavior of Iron in High Purity Water*, Corrosion, vol. 35, pp. 340-344.

- Gilbert, P.T., Oct.–Dec., 1948. *An Investigation into the Corrosion of Zinc and Zinc Coated Steel in Hot Waters*. Sheet Metal Industries.

- Greene, N. D., Bishop, C.R., and Stern, M., 1961, *Corrosion and electrochemical behavior of chromium-noble metal alloys*, Journal of the Electrochemical Society, Vol. 108, No. 9, PP. 836–841.

- Grubb, J., 2009, *High Alloy Stainless Steels for Concentrated Sulfuric Acid*, 5D Corrosion solutions, Conference.

- Guo, J., Seo, M., Sato, Y., Hultquist, G., Leygraf, C., and Sato, N., 1986, *Electrochemical behavior and surface composition of copper containing ferritic stainless steel in sulfuric acid solution*, Corrosion Engineering, Vol.35, PP. 283–288.

- Hasan, B. O., Abdul Kader, H. D., and Abdul-Jabbar, M. F., 2011, *Experimental Study on Carbon Steel Corrosion and its Inhibition Using Sodium Benzoate Under Different Operating Conditions*, Iraqi Journal of Chemical and Petroleum Engineering, Vol.12, No.3, PP.11-24.

- Hasan, B. O., Heat, Mass, and Momentum, 2003, *Analogies to Estimate Corrosion Rates under Turbulent Flow Conditions*, Ph. D. Thesis Dept. of Chem. Eng., University of AL-Nahrain, Baghdad.

- Hermas, A. A., Ogura, K., and Adachi, T., 1995, *Accumulation of copper layer on a surface in the anodic polarization of stainless steel containing Cu at different temperatures*, Electrochimical Acta, vol.40, no.7, PP.837–844.

- Higginson A., Newman R. C., and Procter R. P. M., 1989, *The passivation of Fe-Cr-Ru alloys in acidic solutions*," Corrosion Science, Vol.29 , No.11-12, PP.1293–1318.

- Hubbard, D. W., and Lightfoot, E. N., 1966, *Correlation of Heat and Mass Transfer Data for High Schmidt and Reynolds Numbers*, Ind. Eng. Chem. Vol.5, PP.370–379.

- Ibrahim, M. A. M., Abd El Rehim, S. S. and Hamza, M. M., 2015, *Potentiodynamic polarization behavior of some austenitic stainless steel AISI samples of different molybdenum contents in H_2SO_4 solutions*, Arabian Journal of Chemical and Environmental Research, Vol.2, No.2, PP.37–50.

- Lothongkum G., Chaikittisilp S., Lothongkum A. W., 2003, *XPS investigation of surface films on high Cr-Ni ferritic and austenitic stainless steels*, Appl. Surf. Sci., 218, PP. 203-210.

- Mahato, B. K., Cha, C. Y., and Shemlit, W., 1980, Corrosion Science, Vol. 20, PP. 421-441.

- Nesic, S., Solvi, G. T., and Enerhaug, J., 1995, *Comparison of Rotating Cylinder and Pipe Flow Test for Flow-Sensitive Carbon Dioxide Corrosion*, Corrosion, Vol. 51, PP. 773-787.

- Okamoto, G., 1973, *Passive film of 18-8 stainless steel structure and its function*, Corrosion Science, Vol.13, Issue 6, PP. 471-489.

- Revie, R.W. and Uhlig, H. H., 2008, *Corrosion and Corrosion Control an Introduction to Corrosion Science and Engineering*, fourth edition, John Wiley & Sons, Inc., Hoboken New Jersey.

- Ross, T. K., Wood, G. C., and Mahmud, I., 1966, *The Anodic behaviour of Iron-Carbon Alloys in Moving Acid Media*, J. Electrochem. Soc., Vol. 113, PP. 334-345.

- Shams El-Din, A.M., Wang, L. and Saber, T. M. H., 1994, *Behaviour of High Strength Molybdenum Containing Stainless Steels in Arabian Gulf Water*. Part 1: Oxide Film Thickening. British Corrosion Journal, 29, PP. 58-64.

- Sherif El-Sayed M., 2014, *A Comparative Study on the Electrochemical Corrosion Behavior of Iron and X-65 Steel in 4.0 wt % Sodium Chloride Solution after Different Exposure Intervals*, Molecules, 19, PP. 9962-9974.

- Silverman D.C., 1984, Corrosion NACE, No. 5, Vol. 40, PP. 220.

- Singh, V.B., Ray, M., 2007, *Effect of H_2SO_4 addition on the corrosion behaviour of AISI 304 austenitic stainless steel in methanol-HCl solution*, Int. J. Electrochem.Sci., Vol 2, PP. 329-340.

- Talbot, D. E. J. and Talbot, J. D. R., 1998, *Corrosion Science and Technology, CRC series in materials science & technology*, New York.

NOMENCLATURE

Symbol	Meaning	Units
A	surface area of specimen	mm^2
CR	corrosion rate	$gm/m^2.day$
E_g	galvanic potential	V
$E_{corr.}$	corrosion potential	V
t	immersion time	h
T	temperature	^oC
u	revolution per minute	rpm

ΔW	weight loss	gm

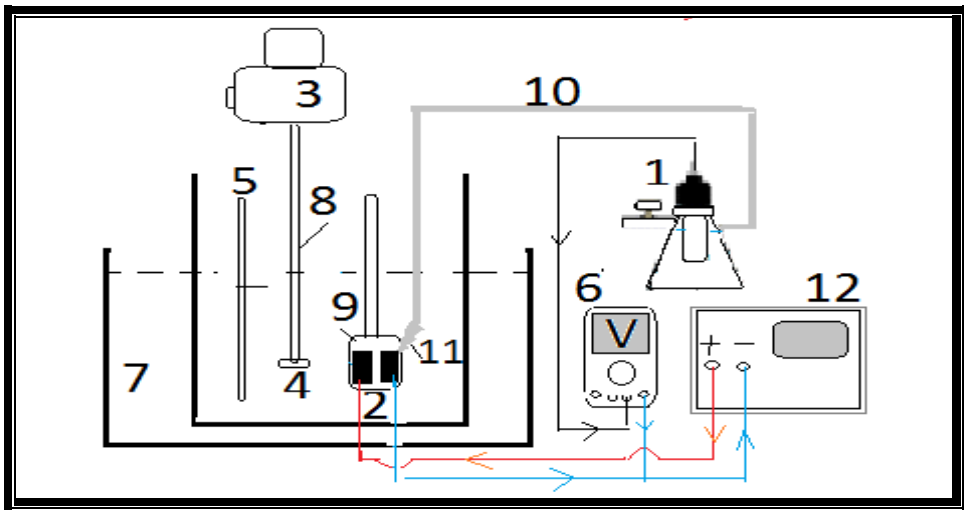

Figure 1. Galvanic experiment set-up: 1- Reference Saturated Calomel Electrode (SCE), 2- Working electrode (specimen), 3-Motor, 4- Stirrer, 5- Thermometer, 6- Voltmeter, 7- Water bath, 8- Glass shift, 9- Holder of specimens, 10- Rubber, 11- Luggen capillary tube, 12- Zero Resistance Ammeter (ZRA).

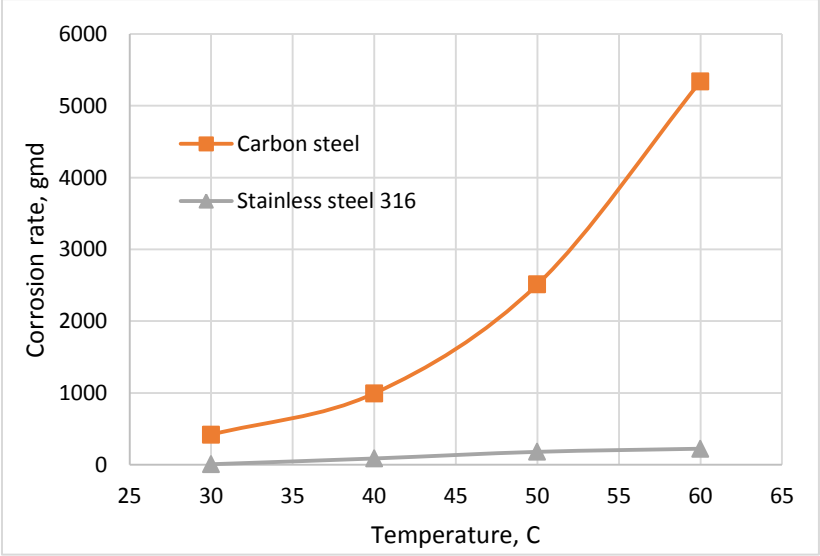

Figure 2. Variation of corrosion rate with temperature at stationary condition.

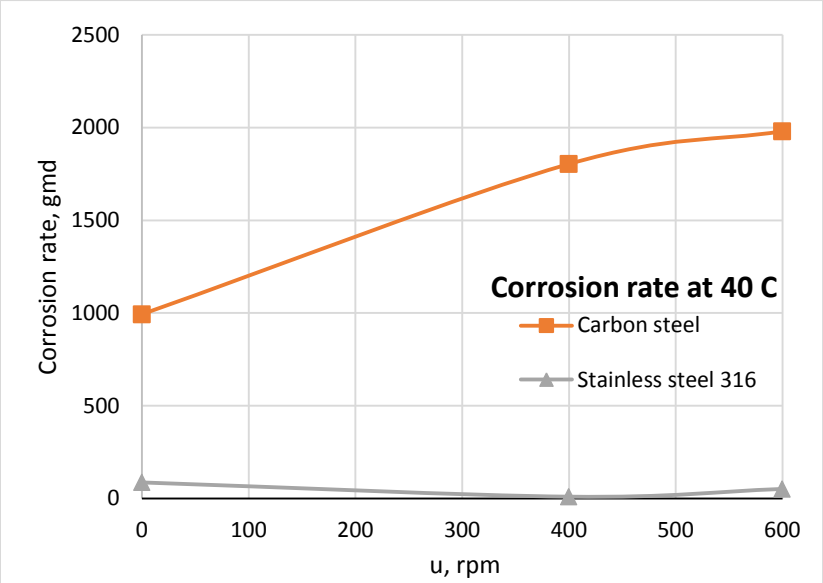

Figure 3. Corrosion rate vs. velocity of CS and SS at T=40 ºC.

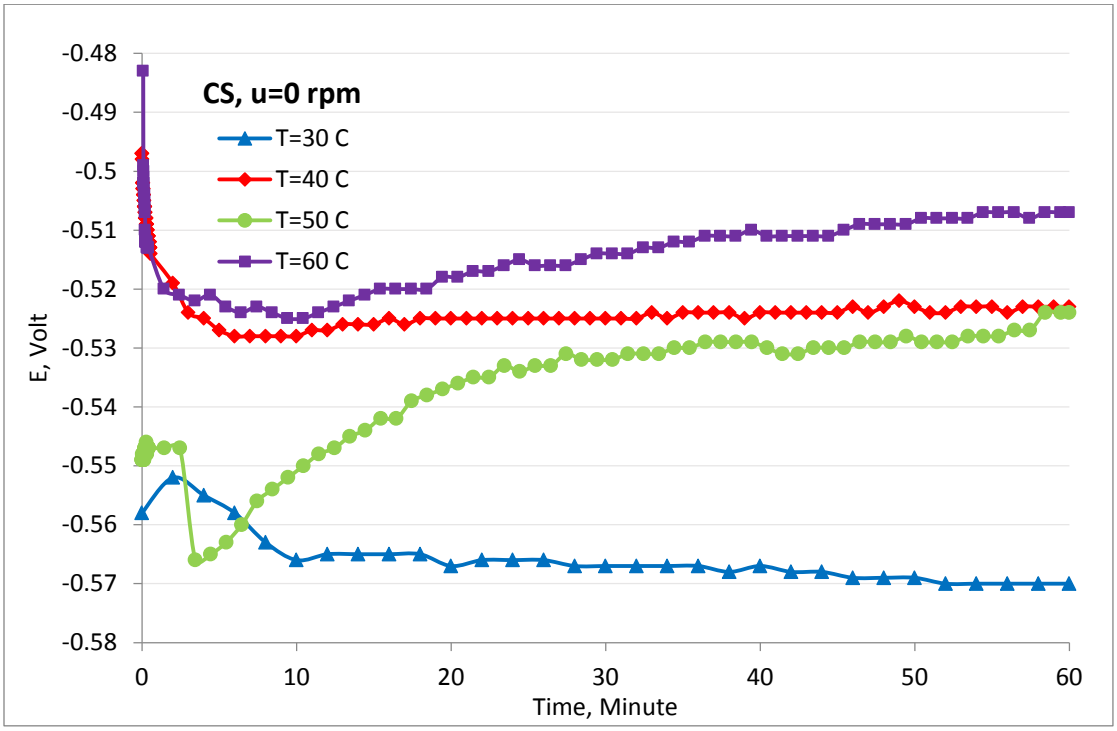

Figure 4. Corrosion potential vs. time of carbon steel specimen at stationary condition at different temperature.

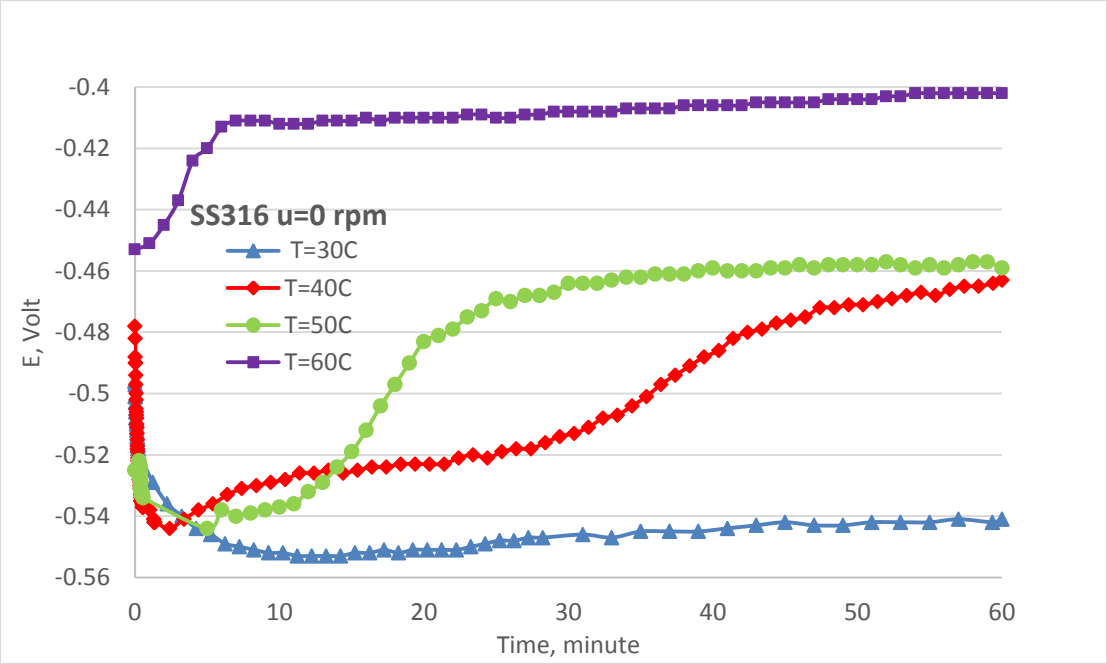

Figure 5. Corrosion potential vs. time of stainless steel specimen at stationary condition at different temperature.

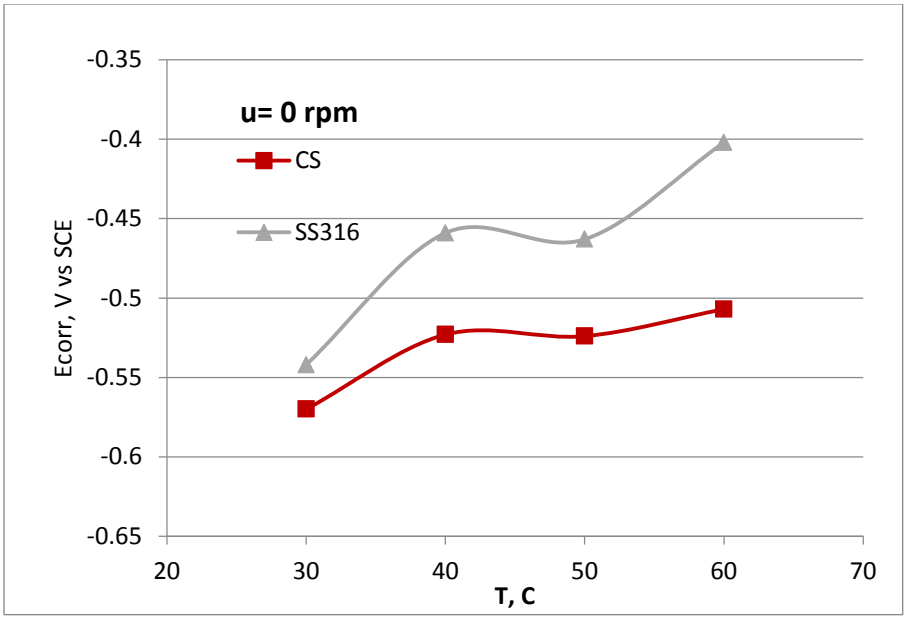

Figure 6. Variation of E_{corr} with temperature at stationary condition.

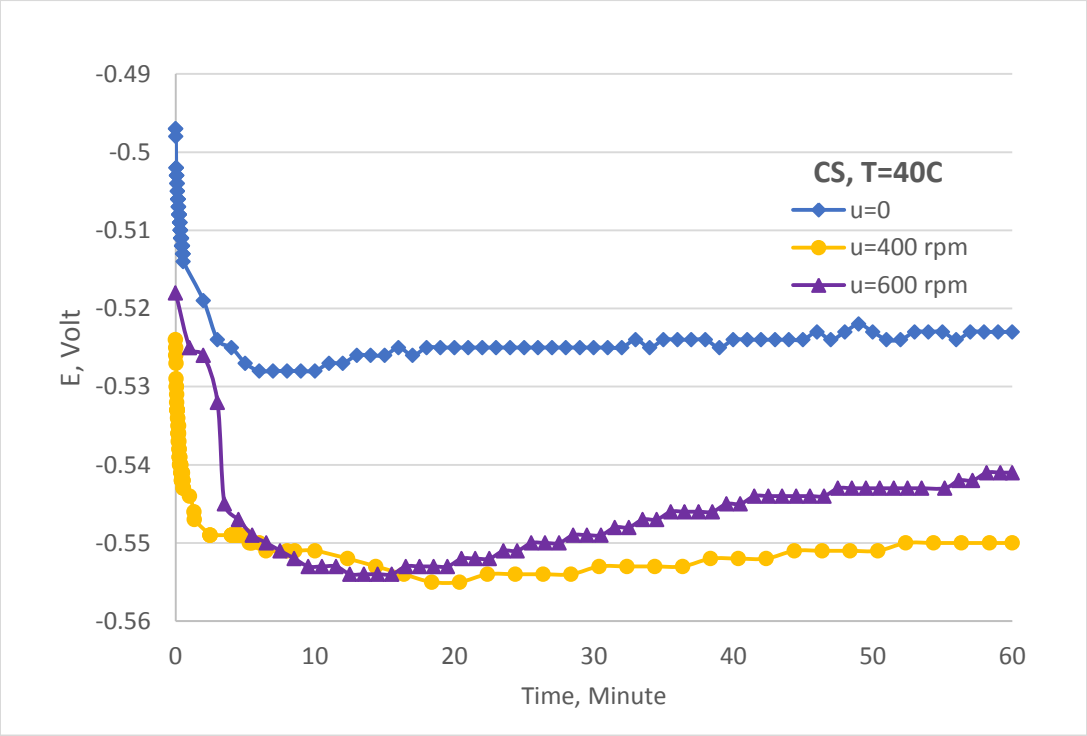

Figure 7. Corrosion potential vs. time of CS at different velocity and 40 ºC.

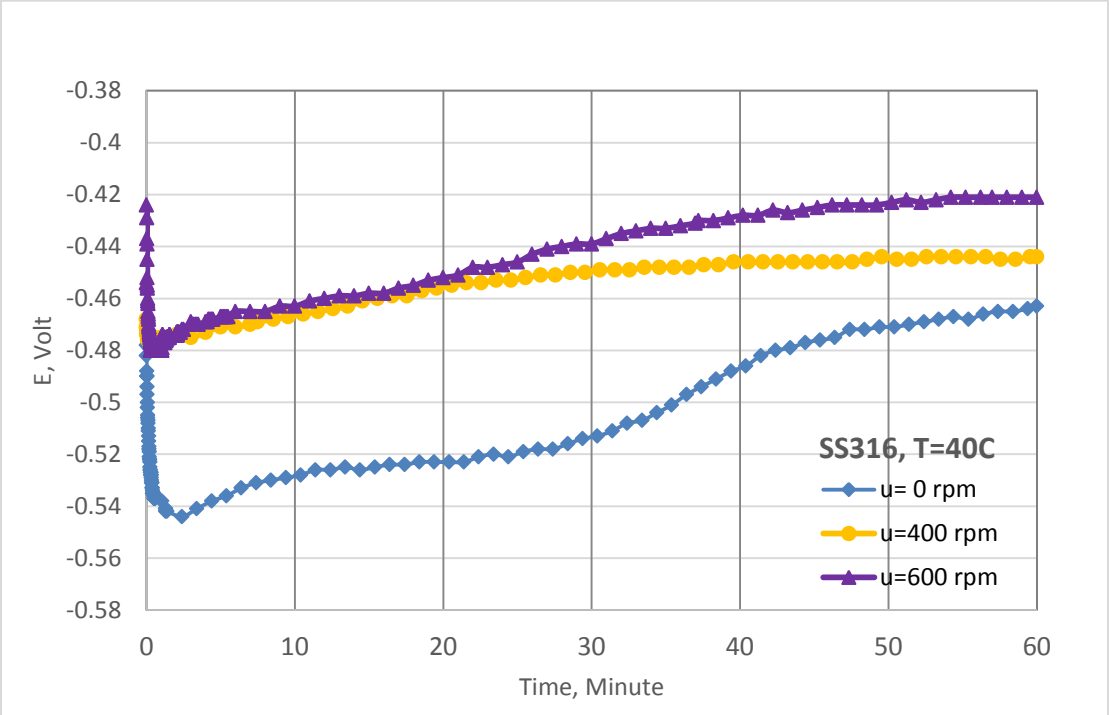

Figure 8. Corrosion potential vs. time of SS316 at different velocity and 40 ºC.

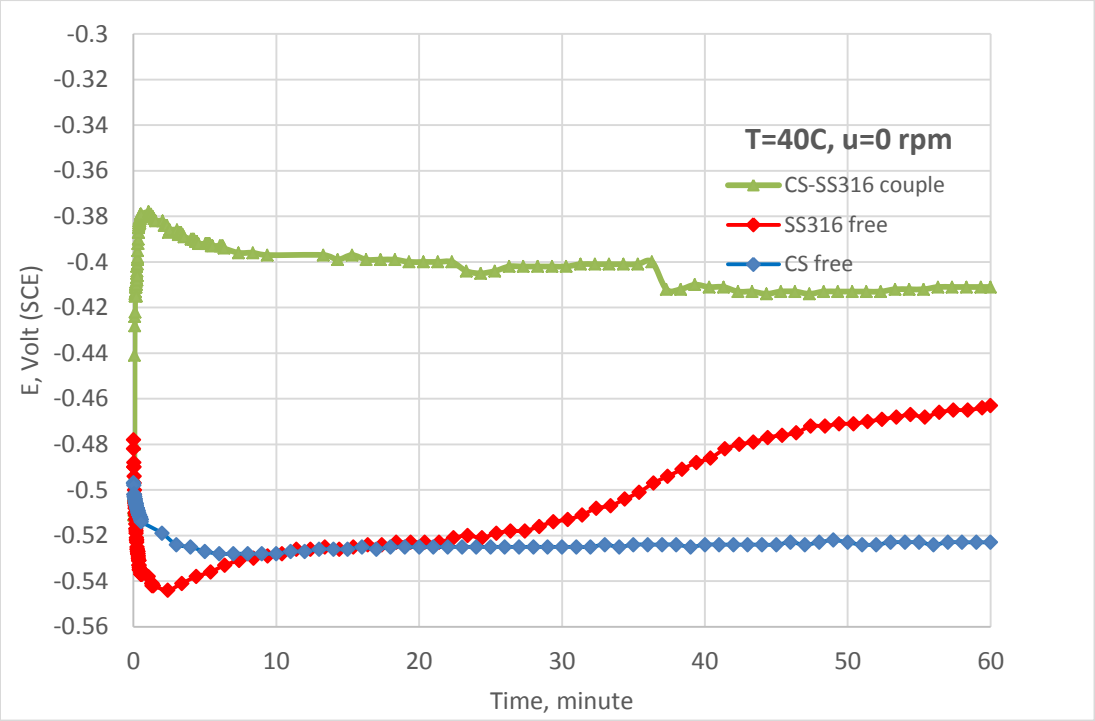

Figure 9. OCP and galvanic potential versus time of carbon steel and stainless steel at const. temperature (T=40 ºC) and stationary (u=0 rpm).

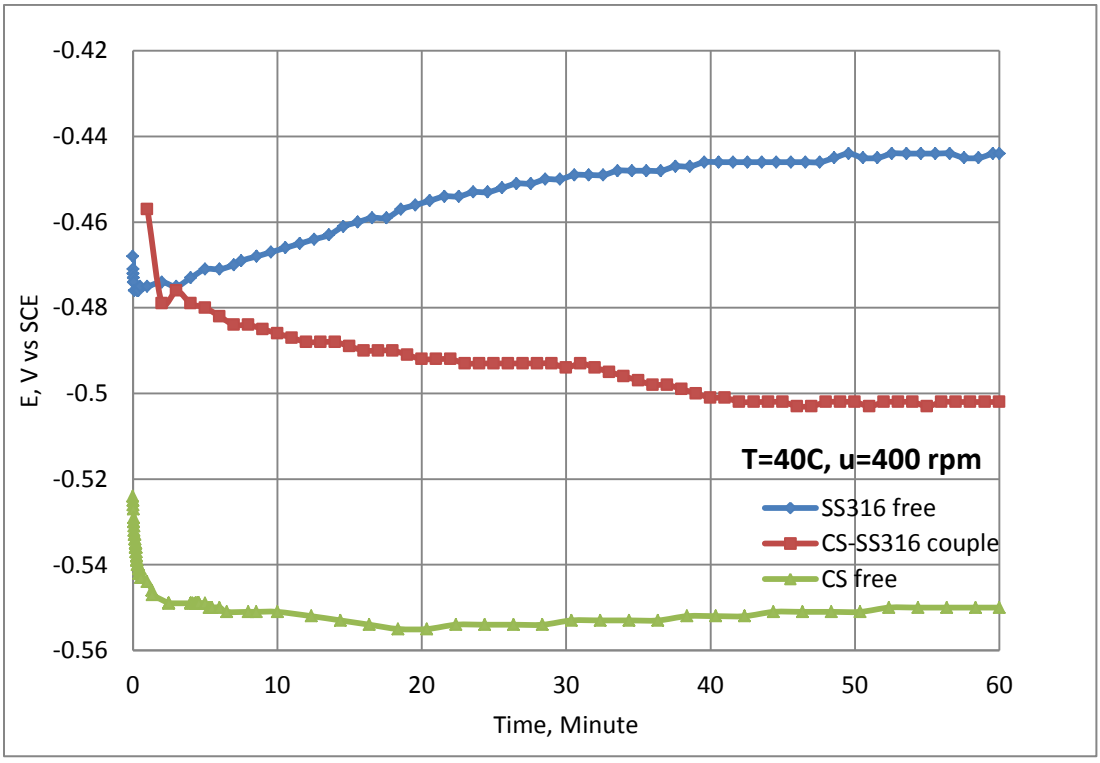

Figure 10. Potentials of CS, SS316, CS-SS316 couple under u=400 rpm.

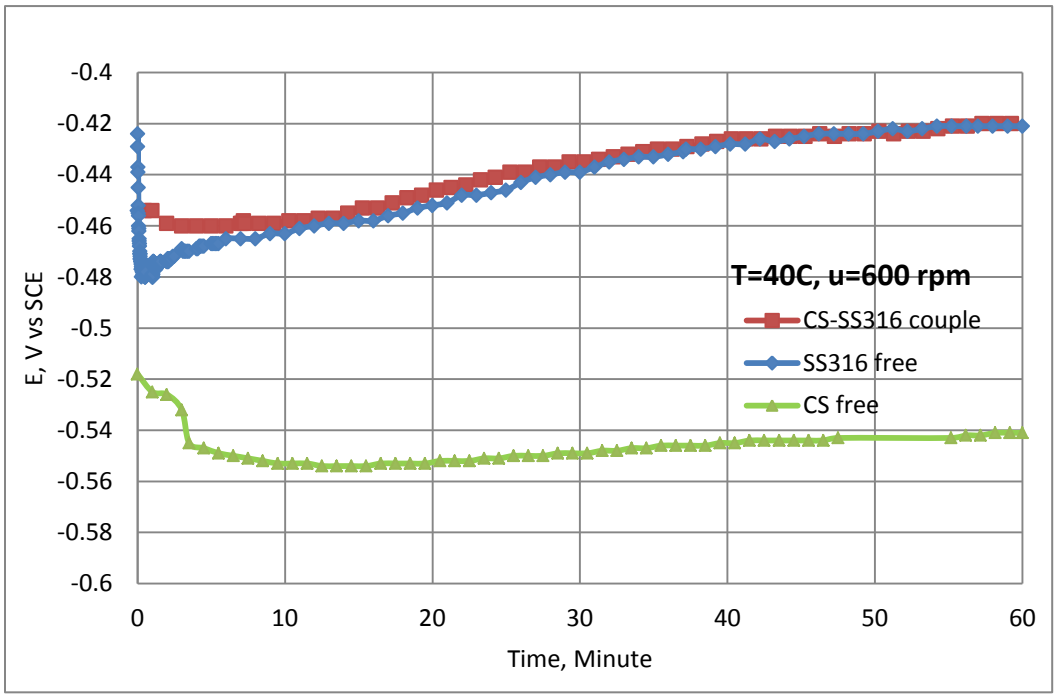

Figure 11. Potentials of CS, SS316, CS-SS316 couple under u=600 rpm.

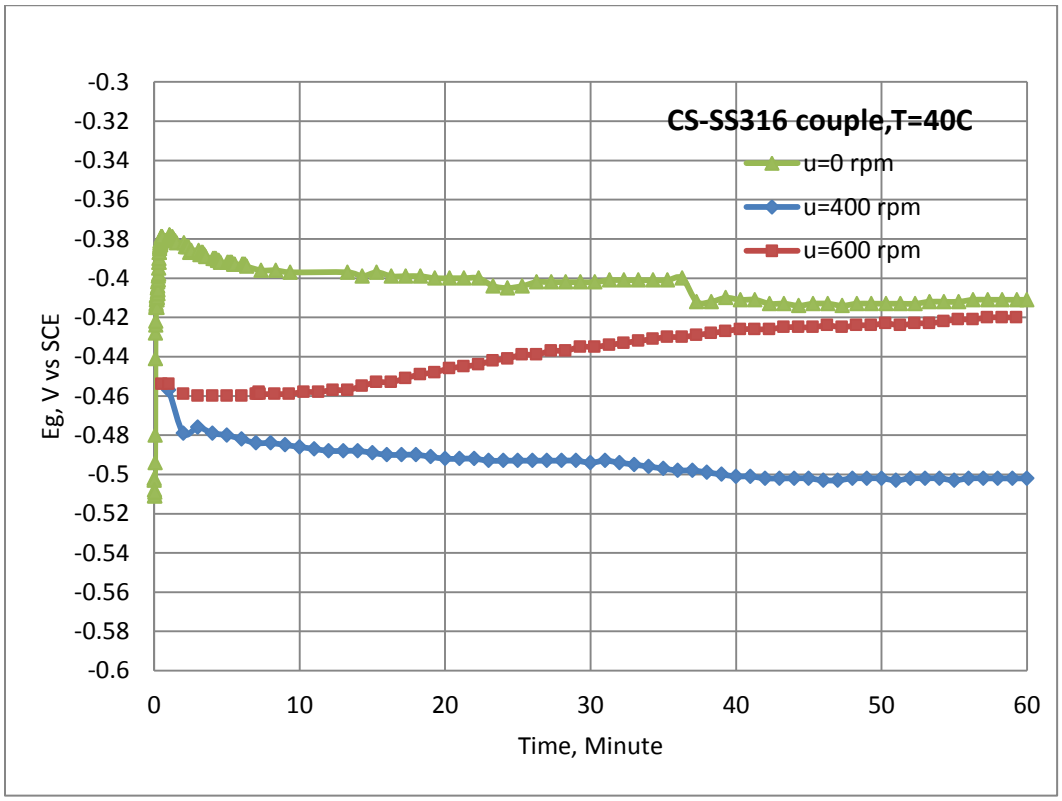

Figure 12. Effect of agitation velocity on the galvanic potential (CS-SS316).

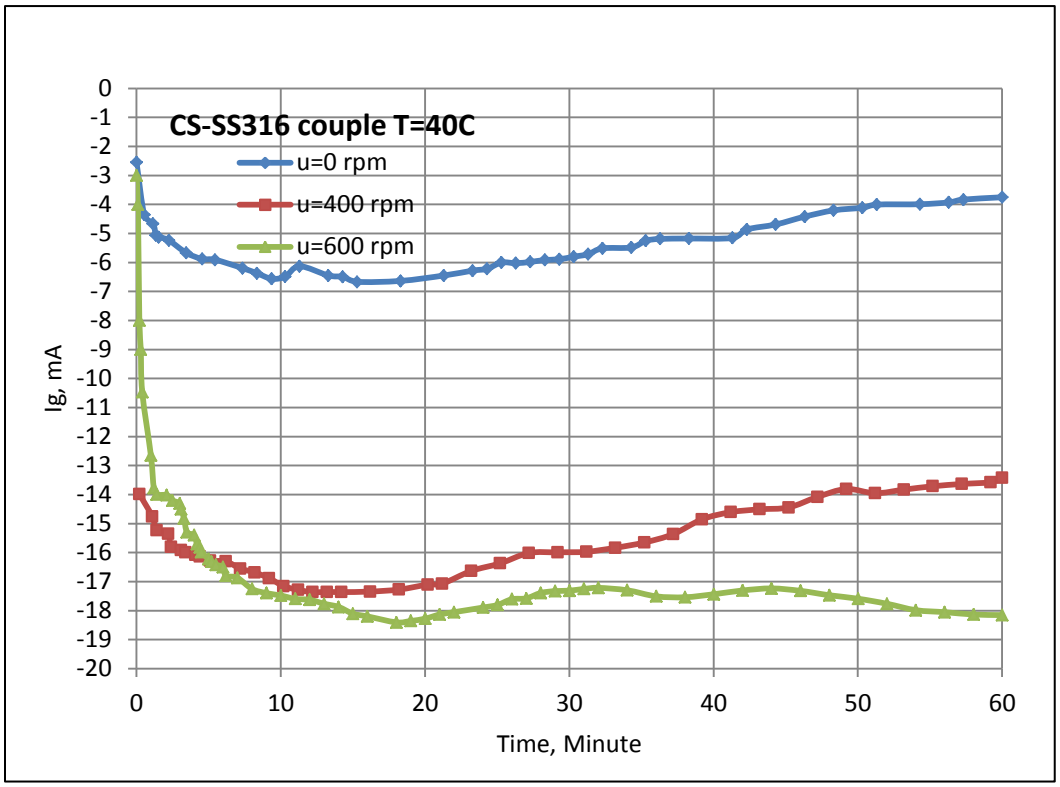

Figure 13. Effect of agitation velocity on the galvanic current (CS-SS316).

Table 1. Analysis of carbon steel specimen

Carbon steel	0.29% C	0.62% V	0.00% Cr	0.22% Mn	0.08% Cu	0.08% Mo	Balance Fe

Table 2 Analysis of stainless steel specimen

Stainless steel 316	0.08% C	2% Mo	16 % Cr	2% Mn	0.08% P	0.03% S	0.75% Si	0.1% N	Balance Fe

Table 3 Corrosion rate of carbon steel and stainless steel 316 in free and coupling at different agitation velocity and T=40 ºC.

u, rpm	***CR, gmd***			
	CS free	***SS316 free***	***Cs(coupled to SS316)***	***SS 316(coupled to CS)***
0	993.4	86.3414	1148.43	22.2996
400	1803.48	9.4736	1803.786	0
600	1980	51.2195	1896.296	8.3623